THE ANATOMICAL RECORD 292:1397–1405 (2009)

Biomechanics of Dromaeosaurid Dinosaur Claws: Application of X-Ray Microtomography, Nanoindentation, and Finite Element Analysis

PHILLIP L. MANNING,[1,2*] LEE MARGETTS,[1,3] MARK R. JOHNSON,[4] PHILIP J. WITHERS,[4] WILLIAM I. SELLERS,[5] PETER L. FALKINGHAM,[1] PAUL M. MUMMERY,[4] PAUL M. BARRETT,[6] AND DAVID R. RAYMONT[7]

[1]School of Earth, Atmospheric and Environmental Sciences, and The Manchester Museum, University of Manchester, Manchester, United Kingdom
[2]Department of Earth and Environmental Sciences, University of Pennsylvania, Philadelphia, Pennsylvania
[3]School of Computer Science, University of Manchester, Manchester, United Kingdom
[4]School of Materials, University of Manchester, Manchester, United Kingdom
[5]Faculty of Life Sciences, The Mill, University of Manchester, Manchester, United Kingdom
[6]Natural History Museum, London, United Kingdom
[7]School of Engineering, Computing and Mathematics, University of Exeter, Exeter, United Kingdom

ABSTRACT

Dromaeosaurid theropod dinosaurs, such as *Velociraptor*, possess strongly recurved, hypertrophied and hyperextensible ungual claws on the pes (digit II) and manus. The morphology of these unguals has been linked to the capture and despatching of prey. However, the mechanical properties or, more importantly, the mechanical potential of these structures have not been explored. Generation of a 3D finite element (FE) stress/strain contour map of a *Velociraptor* manual ungual has allowed us to evaluate quantitatively the mechanical behavior of a dromaeosaurid claw for the first time. An X-ray microtomography scan allowed construction of an accurate 3D FE mesh. Analogue material from an extant avian theropod, the pedal digit and claw of an eagle owl (*Bubo bubo*), was analyzed to provide input data for the *Velociraptor* claw FE model (FEM). The resultant FEM confirms that dromaeosaurid claws were well-adapted for climbing as they would have been resistant to forces acting in a single (longitudinal) plane, in this case due to gravity. However, the strength of the unguals was limited with respect to forces acting tangential to the long-axis of the claw. The tip of the claw functioned as the puncturing and gripping element of the structure, whereas the expanded proximal portion transferred the load stress through the trabeculae and cortical bone. Enhanced climbing abilities of dromaeosaurid dinosaurs supports a scansorial phase in the evolution of flight. Anat Rec, 292:1397–1405, 2009.

Key words: dromaeosaur; theropod; ungual; finite element analysis

Grant sponsor: Engineering and Physical Sciences Research Council in the United Kingdom (finite element modeling); Grant numbers: EP/F055595/1, EP/D037867/1.

*Correspondence to: Phillip L. Manning, School of Earth, Atmospheric, and Environmental Sciences, and The Manchester Museum, University of Manchester, Oxford Road, Manchester, M139PL, United Kingdom. Fax: +44(0)161 306 9360. E-mail: phil.manning@manchester.ac.uk

Received 9 June 2009; Accepted 9 June 2009

DOI 10.1002/ar.20986
Published online in Wiley InterScience (www.interscience.wiley.com).

INTRODUCTION

Predatory dinosaurs (Theropoda) were diverse and successful animals during the Mesozoic Era and are currently represented in modern ecosystems by their direct descendants, the birds (Holtz and Osmólska, 2004; Vargos and Fallon, 2004; Pennisi, 2005). Nonavian theropods ranged in size from the tiny *Microraptor zhaoianus* (with a trunk length of only 47 mm) to the huge *Tyrannosaurus rex* (up to 14 m in length) (Holtz and Osmólska, 2004). The theropod clade that forms the focus of this study, Dromaeosauridae (Matthew and Brown, 1922), was an obligatory bipedal group of lightly-built cursors (estimated live weight from 20 to 80 kg) that were close to avian ancestry (Norell and Makovicky, 2004). Dromaeosaurid limbs exhibit numerous anatomical specializations including long raptorial hands with three functional digits, highly mobile hand-wrist elements, unique caudal vertebrae with highly elongate prezygapophyses adapted to assist balance, and a recurved, hypertrophied and hyperextensible claw on pedal digit II (Ostrom, 1969, 1990). The functional and palaeobiological significance of the strongly recurved manual ungual of the Late Cretaceous Asian dromaeosaurid *Velociraptor* (Norell and Makovicky, 1999) forms the subject of this article.

Dromaeosaurid unguals are commonly interpreted as weapons for disemboweling (with pedal unguals) or capturing/manipulating (with manual unguals) large-bodied prey, such as iguanodontian ornithopods (Ostrom, 1969). The effectiveness of the enlarged pedal digit II ungual as a disemboweling implement has been challenged by recent experiments using a hydraulic reconstruction of a dromaeosaurid hind limb (Manning et al., 2006). However, the mechanical behavior of dromaeosaurid claws while under load has not been satisfactorily explored.

Homologous structures in the feet of extant perching/climbing birds provide useful insights into the palaeobiology, evolution, form and function of dromaeosaurid claws. However, an understanding of the microarchitecture and 3D properties of dromaeosaurid unguals would provide a more robust interpretation of their biomechanical function with the potential to provide new insights into behavior. To determine the displacements (deformations), strains (displacement gradients), and stresses (force intensities) that result from subjecting dromaeosaurid claws to loads, it was necessary to generate a finite element model (FEM).

Finite element analysis (FEA) provides a useful technique to quantitatively analyze complex 3D biological systems. However, the physical properties of the material being modeled must be known if realistic FEMs are to be generated. Mineralized fossil material cannot be used to determine the original material properties of a bone (Young's modulus, Poisson's ratio, etc.) so it is necessary to identify suitable modern analogue material. Moreover, specifying biomaterial properties for FEA is difficult as they can vary within the structure under investigation according to location (inhomogeneous materials), the directions in which forces are applied (anisotropic behavior), the loading rate (as occurs in poroelastic and viscoelastic materials), and the magnitude of the load (which can lead to nonlinear effects) (Beaupre and Carter, 1992). We constrained the biomaterial specifications used in this study using both evolutionary and functional cues.

Claw form and function varies widely among vertebrates, however, claw sheath composition does not. Claw sheaths, nails, and hooves are composed of keratin, a strong, fibrous protein (Raven and Johnson, 1992). Keratin protects the bone of the terminal phalanx and assists in providing traction during climbing, prey capture, and occasionally killing [brief review in Manning et al., (2006)]. The morphology of dromaeosaurid unguals, combined with rare soft tissue preservation (Clark et al., 1999), indicates that theropod claws would have been similarly protected. Extant Phylogenetic Bracketing [EPB: Witmer (1995)] can be used to reconstruct the structure and properties of the keratin claw sheaths possessed by nonavian dinosaurs. Mammal claw sheaths are composed of α-keratin (helical), but bird and reptile claws are composed of β-keratins (pleated-sheet) (Fraser and MacRae, 1980). As nonavian dinosaurs fall within the EPB formed by birds and crocodilians and leave similar osteological traces (attachment grooves) it is likely that the claw sheaths of these animals were also composed of β-keratin (Manning et al., 2006).

The keratinous claw sheath is strongest mechanically along its parasagittal plane (Vincent and Owers, 1986; Bonser, 2000), representing a function of the microstructural arrangements of the individual keratin fibers (Beaupre and Carter, 1992). A requirement of all biological materials subject to loading is that stresses are kept within safe limits (Alexander, 1981), and it is likely that the claw sheath and ungual phalanx of dromaeosaurid manual claws would have had similar safety limits to those of extant raptorial falconiform and strigiform birds. Similarities between dromaeosaurid and owl claw morphology are striking, in terms of both internal and external anatomy. Comparable distributions of cortical and trabecular bone in these taxa allow confident reconstruction of the mechanical properties of dromaeosaurid claws.

MATERIALS AND METHODS

Fossil Material

A manual ungual of *Velociraptor mongoliensis* (Manchester Museum, University of Manchester, specimen LL.12392) was Computed tomography (CT) scanned to provide a 3D dataset for the finite element (FE) mesh (see below for details). *V. mongoliensis* is known primarily from the Djadokhta Formation (Campanian) of Mongolia (Osborn, 1924). *Velociraptor* is closely related to *Deinonychus* and *Dromaeosaurus*; however, it is distinguished from all other dromaeosaurids by its relatively long, low skull and depressed muzzle (Sues, 1977).

Extant Material

A subadult/juvenile eagle owl (*Bubo bubo*) from the biological sciences collections, University of Manchester, was used in this study. The bird had a frozen weight of 1996 g. *Bubo bubo* is a member of the family Strigidae, which consists of all the typical owls (Penteriani et al., 2002).

A fully-intact terminal ungual phalanx and part of the adjacent phalanx, both from pedal digit III of the right pes, were amputated from the Eagle Owl (Fig. 1). The bones, along with all the associated soft tissue were

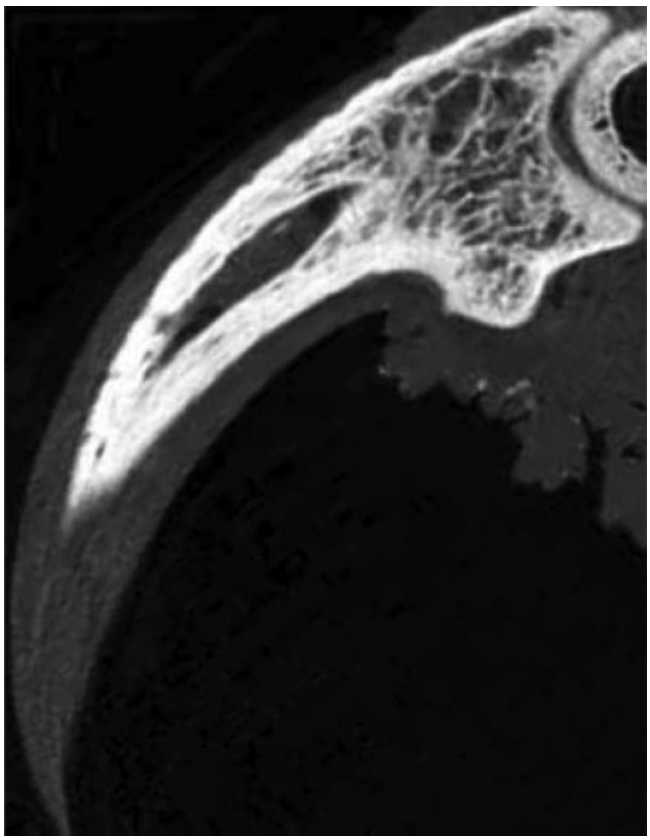

Fig. 1. High-resolution x-ray CT of owl terminal ungual phalanx and pedal claw (bone core and keratin sheath). Bone is white, keratin, and soft-tissue are grey.

nano-indented to provide input data for the FE mesh of the CT scanned *Velociraptor* claw (Table 1).

Claw Geometry

The arc for both the *Velociraptor* and owl claws were measured using Feduccia's (1993) method (Fig. 2).

A perpendicular (CD) is drawn to bisect the chord (AB) of the inner arc, which is bisected at point X. Perpendiculars are drawn to bisect the chords AX and XB. These perpendiculars when extended, meet at the center (E′) of the circle of which the arc is part. The radii are then drawn to each end of the arc (AE′ and BE′). The angle (Y) between these radii is a measure of the degrees of arc (Feduccia, 1993).

X-ray Microtomography

X-ray micro-tomography (XMT) is a nondestructive evaluation technique that allows the internal structure of an object to be imaged by reconstructing the spatial distribution of the local linear X-ray absorption coefficients of the materials/phases contained within. This provides a virtual 3D representation of the internal architecture of an object from which two-dimensional (2D) cross-sectional slices can be extracted along the three orthogonal planes of the object (Elliott and Dover, 1982; Marrow et al., 2004; Babout et al., 2005). In conventional radiography, the image plane is approximately normal to the X-ray beam, and the image represents total X-ray attenuation through the object. CT computes a 3D digital representation from a series of 2D X-ray radiographs taken around a single axis of rotation, or a 2D slice perpendicular to the axis of rotation for 1D line detector (fan beam geometry). The digital image is stored as an array of numbers representing local X-ray attenuation values for each of the small volumetric pixels (voxels) that make up the slice, these attenuation data are represented in the reconstructed image as a series of grey scale values. By thresholding the volume so as to associate different grey levels with different materials the 3D object can be converted into a microstructurally faithful 3D mesh suitable for FEM describing the geometry of each constituent. Once each phase has been ascribed mechanical properties, it is possible to predict the loads experienced throughout a body according to its exact size, shape and volume.

Measurements were carried out using a high-resolution computerized tomography and digital radiography system (HMXST 225) from X-Tek Systems Ltd., employing a microfocus X-ray source (5 μm focal spot size) capable of tube potentials up to 225 kV. The imaging arrangement is based on cone beam geometry. In such an arrangement, the voxel resolution of the reconstructed 3D volume depends on the source-to-object distance. The object was placed on a manipulator situated between the X-ray source and the detector system (consisting of image intensifier and CCD), providing magnification and rotation for collection of 470 radiographs over 180°. The radiographs were collected using a tube potential of 50 kV with a tungsten anode target giving an approximately 5 μm point source. To shape the energy spectrum of the X-ray beam, and thus improve the image quality in the reconstructed slices (i.e., increasing the signal-to-noise ratio), a 0.25 mm thick copper X-ray filter was placed just behind the point source and in front of the sample during image acquisition. This filter removes low-energy photons from the polychromatic beam, thus minimizing artefacts (noise) in the reconstructed slices and the distribution of voxels with different intensities. The 3D tomographic volumes were reconstructed using a cone beam extension of the filtered backprojection algorithm developed for fan beams (Kak and Slaney, 1987; Youssef et al., 2005) 32 frames were averaged for each of the 470 projections (using an exposure time for each frame of 120 ms). The raw 3D volume had a pixel resolution of 17 μm, reconstructed at a quarter of maximum resolution for easier data manipulation during the subsequent meshing routine.

In situ Compression

Considering the EPB method (Witmer, 1995), bone and keratin samples were collected from the pes of an eagle owl (*Bubo bubo*). The micromechanical properties of the keratin layer and cortical bone of the eagle owl claw were determined from force displacement curves generated by an MTS XP nanoindenter with a Berkovich diamond indenter (Kanari et al., 1997a,b).

TABLE 1. Experimental imaging parameters for scanning the *Velociraptor* claw

X-ray tube: energy, intensity		Radiograph acquisition			Volume reconstruction	
Voltage (kV)	Current (mA)	Rotation (degrees)	Exposure time (msec)	Number of frames/angle	Voxel size (μm)	Reconstructed volume (voxels)
50	0.135	0.4	120	32	17	256 × 256 × 470

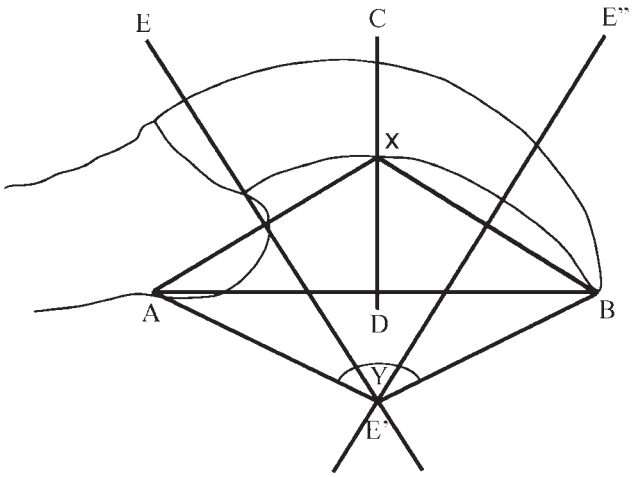

Fig. 2. Claw curvature measurements (after Feduccia, 1993).

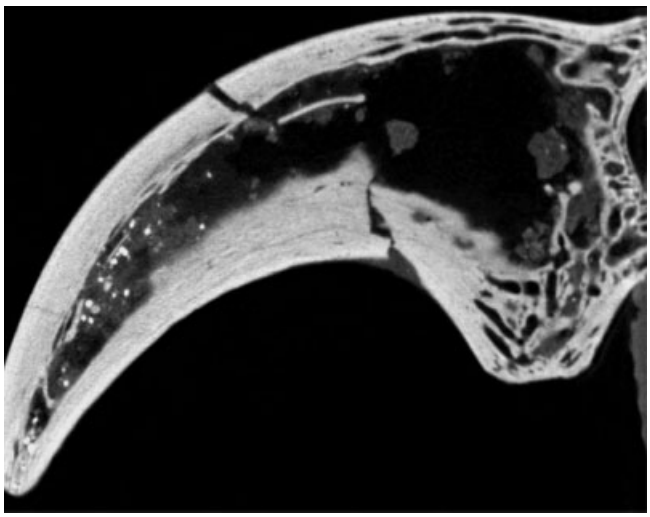

Fig. 3. XMT cross-section of the *Velociraptor* (LL. 12392) manual claw showing the main biomaterial phases (trabecular and cortical bone).

Finite Element Model

A microstructurally faithful FE mesh of the *Velociraptor* ungual was created in 3D directly from the raw tomography images using the ScanIP™ and ScanFE™, commercial packages from Simpleware Ltd. The image threshold values used for segmentation (the process of discriminating between the various structures from the image) were selected according to estimates for the volume fractions of cortical bone, trabecular bone, and porosity. The CT imaging conditions used are summarized in Table 1.

In FEA, individual FEs can be of any shape. However, with voxel image data, it is most convenient to use brick elements which, when they are perfect cubes, are the FE analogue of voxels. A one-to-one correlation between brick elements and voxels would lead to an FE mesh several orders of magnitude larger than can be processed using the Abaqus software. Therefore, the model was down-sampled to allow the analyses to run on a desktop computer. The resultant FE mesh contains ~500,000 elements rather than 30 million voxels. Care was taken to ensure that the simplified mesh still captured the detail of the claw microstructure. A further simplification for this preliminary model was to ignore the keratin layer on the outer surface of the claw, with the focus being on the modeling of the cortical and trabecular bone, with a true representation of porosity in the structure (Fig. 3).

Loading: Stress/Strain Analysis

A FE mesh was created to represent the entire ungual (Fig. 4). The original fossil (Fig. 3) is fractured through the middle and the two pieces have been glued together, slightly out of alignment. Before the FE mesh was generated, the two pieces of the claw were digitally realigned, and the fracture was removed. The latter was achieved by inflating the volume so that the fractured surfaces healed. The volume was then returned it to its original shape by reversing the inflation procedure, while algorithmically enforcing the continuity of the surface across the original fracture zone, preventing the fracture from reappearing.

Figure 4 shows where the loads and boundary conditions were applied to the mesh. The aim was to recreate the likely forces experienced by the claw in use, during prey capture, climbing, etc. A distributed force was applied over a surface area representative of the attachment site for the flexor tendon. The initial force of 400N was calculated using the approximate weight of *Velociraptor* as a guide [Manning et al., (2006)]. The FE mesh was subjected to a linear elastic analysis using ABAQUS CAE 6.6 with the input data being determined by nanoindentation and from literature (above).

RESULTS

Claw Geometry

The *Velociraptor* manual ungual modeled in this study (minus its keratinous sheath) possessed a claw arc measurement of 127°.

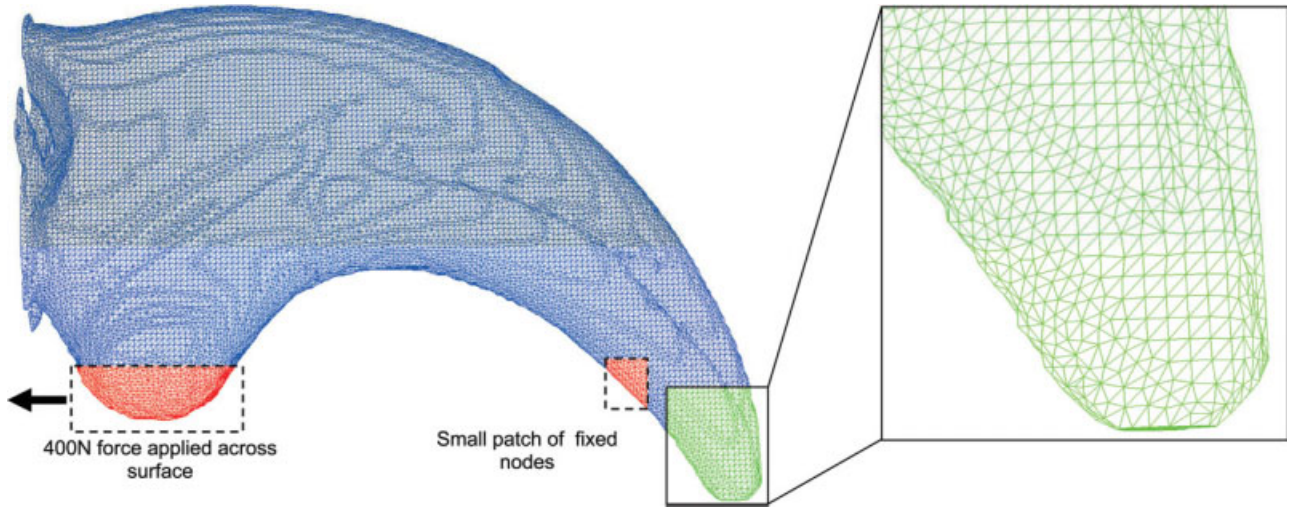

Fig. 4. 3D finite element mesh of the *Velociraptor* claw, showing boundary conditions and close-up detail of the mesh (inset).

TABLE 2. Input data derived from the eagle owl claw (*Values taken from literature: (Van Ruijven et al., 2002)

Region indented	Number of indents	Mean modulus (GPa) to 1.d.p.
Keratin layer	10	6.8 (±1.5)
Cortical bone	11	21.1 (±2.3)
*Trabecular bone	–	19.0

In situ Compression

Reliable indentation properties could not be obtained for the trabecular bone due to its highly porous nature; values for this were obtained from the literature (Van Ruijven et al., 2002). The indenter tip was moved at a rate of ~5 nm s^{-1} to a chosen cross-sectional area of the eagle owl claw and contact between the two determined at a specific applied load. The indentation was conducted at a load range from 0 to 60 μN. Ten different points were indented at each load for the keratin layer and eleven different points indented for the cortical bone. The results derived from the loading–unloading cycles are shown in Table 2.

Note: the Poisson's ratios used were: 0.3, 0.32, and 0.2 (Kitchener and Vincent, 1987; Van Ruijven et al., 2002) for the keratin, cortical and trabecular phases, respectively. These values were employed for subsequent FEM using a commercial FEM package (Abaqus).

XMT and Finite Element Model

Variation in bone density and microstructure (trabecular versus cortical bone) has an important influence on a system's stiffness and strength (Carter and Hayes, 1977). Differences in density and microstructure, when coupled with the anisotropic properties of bone (trabecular and cortical) and keratin, leads to a complex composite system that is difficult to model. However, the cortical and trabecular bone in the *Velociraptor* ungual displays a distinct structural orientation that is perpendicular to the ungual long-axis that can be modeled using high element count FEA (Fig. 5). Currently there is no way of modeling element-by-element anisotropy and within each FE isotropy has been assumed.

Model values for the Young's modulus (summarized in Table 2) and Poisson's ratio (Kitchener and Vincent, 1987; van Ruijven et al., 2002) were assigned isotropically to the elements that represented the cortical and trabecular phases of FE meshes. Upon applying the loading conditions shown in Fig. 4, the stress contour plots illustrated in Fig. 6 were obtained.

The initial force of 400N applied to the ungual was deduced from the approximate weight of the *Velociraptor* (Manning et al., 2006). It would be fair to assume that the stresses generated at this load provide a reasonable baseline for assessing the loads that would be encountered when a dromaeosaur used its claws to grasp, lift, and climb. In the living animal, several factors would affect the intensity and distribution of load over the claw/substrate contact and its transmission through the internal microstructure of the claw. For example, the mechanical behavior of living tissues (flexibility, strength at different strain rates) is more complicated than has been used here. That coupled with the rate of ascent when climbing would also affect the values of peak loads.

The maximum value of stress generated by the FEM under the assumed loading conditions, with a force of 400N, is around 60 MPa. This is much less than the typical range of values reported in the literature for the failure stress of extant claws of 150–200 MPa, indicating that it is reasonable to assume that the *Velociraptor* would have been able to support its weight on a very small contact surface while climbing.

It should be noted that the model chosen to represent material behavior in the current study does not include a failure criterion. Therefore, it may be of interest for future work to carry out experimental tests such as three-point bending of the eagle owl claw. This would give an estimate of the failure strength (i.e., ultimate

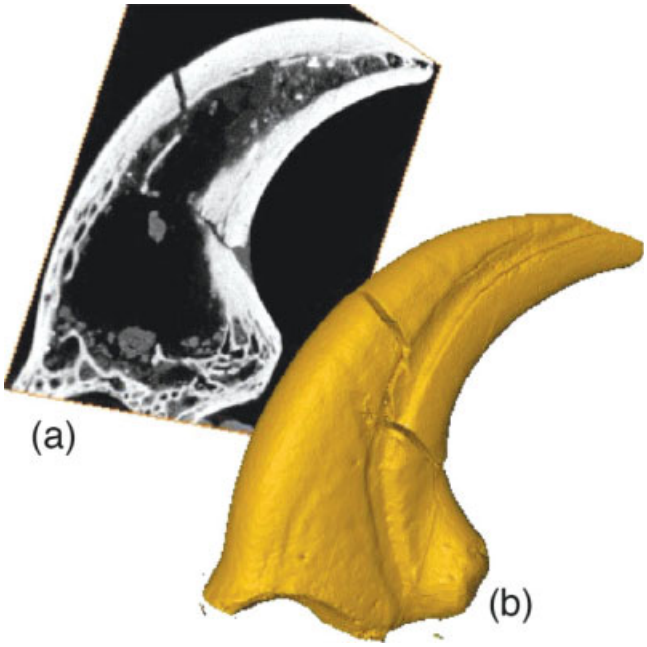

Fig. 5. *Velociraptor* claw comprized of cortical and trabecular bone and true porosity (**a**) 2D tomographic slice (**b**) 3D representation using AMIRA software.

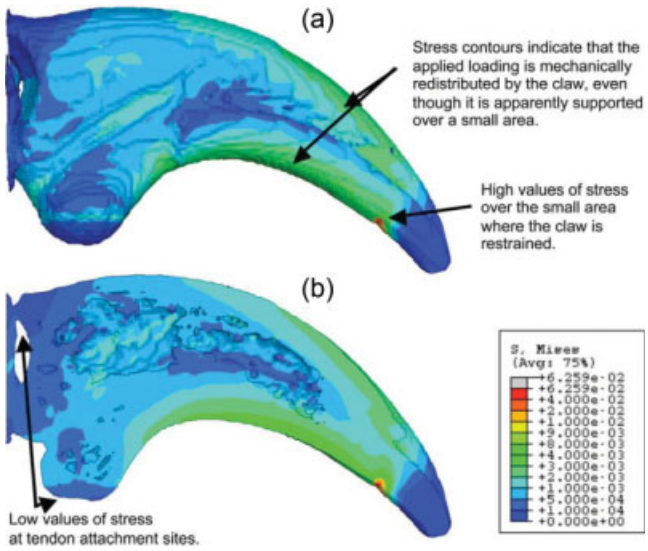

Fig. 6. Contour map of Mises stress (units in GPa) on (**a**) the outer surface of the claw and (**b**) through the mid-section.

limit load) of the *Velociraptor* ungual over a range of different scenarios.

DISCUSSION

The claw geometry of mammals and birds (both pedal and manual) correlates well with arboreal and terrestrial habitats. In a study of over 500 species of birds, Feduccia (1993) demonstrated that modern ground and tree-dwelling birds could be distinguished on the basis of pedal claw curvature. The claw arc measurements for ground birds ranged from 52.2 to 77.6°, those of perching birds from 101.8 to 125.3°, and those of trunk-climbers form 129.5 to 161.6° (Feduccia, 1993). The ungual phalanges on pedal digit II of most dromaeosaurids are large, narrow, pointed, and strongly curved with lateral grooves for the claw sheath. That of *Deinonychus antirrhopus* (YPM 5205) possesses an inner arc measurement of 160° (Ostrom, 1969). Comparisons with extant birds therefore support a climbing function for this structure. Although a climbing/grappling function for the dromaeosaurid pedal digit II ungual during predation has been suggested, it may also have provided assistance during arboreal activity (Chatterjee, 1997; Manning et al., 2006). The *Velociraptor* manual ungual modeled in this study (minus the keratinous sheath) possessed a claw arc measurement of 127°. It is likely that this claw arc angle would increase by 10–15% with the addition of a keratinous sheath, meaning the claw would fall comfortably within Feduccia's (1993) perching and trunk-climber bracket. This adds further support to the proposal that dromaeosaurids might have used their claws to assist climbing behavior (Chatterjee, 1997; Manning et al., 2006).

The central hypothesis regarding claw function in this study was based upon both internal and external pedal morphology. The role of the FE analysis was to test the relationship of form and function, from an engineering point of view. The preliminary study was carried out using the microtomographic scan of the *Velociraptor* manual claw, given limited access to complete pes unguals. The findings from this study can be compared with pes claws, on the basis of geometric and architectural similarity (Manning et al., 2006), with only slight variation in morphology. Pes claws are typically larger than those of the manus, meaning that it could sustain larger loads than those subjected to the model used in the current simulation. The biomechanical function of morphologically comparable structures of similar geometry, but dissimilar size, should behave in a dynamically similar fashion (Alexander, 1989). Future work will apply the methods from this study, by using a pedal ungual phalanx of *Deinonychus* (Ostrom, 1969) to test this hypothesis further.

Many birds are successful climbers, using their feet, tails, beaks, and, in the case of the South American hoatzin (*Opisthocomus hoazin*), their forelimbs while fledglings (Dominguez-Bellom, 1994). The tail feathers of some birds (woodpeckers, woodhoopoes, woodcreepers, treecreepers, and some species of ovenbirds) can provide additional support (McFarland et al., 1979). Ostrom (1969) suggested that dromaeosaurs possessed a reversed hallux, but more recent work (Norell and Makovicky, 1999) has indicated that this reduced digit was positioned craniolaterally and high on the metatarsus.

Ostrom (1969) noted that the recurved shape of the *D. antirrhopus* "killing claw" coincided with the axis of maximum force that could be delivered and concluded that it was adapted for penetrating the flesh of prey. Carpenter (1998) suggested that this morphology was able to provide a piercing function. This study supports both interpretations, but suggests this piercing ability

Fig. 7. The 'fighting pair' *Velociraptor* and *Protoceratops* (IGM 100/25).

did not facilitate the disemboweling of prey, but was instead involved in scansorial behavior.

The force generation of a limb is always primarily to oppose gravity. Thus a dromaeosaur on a horizontal surface needs to generate a primarily vertical force by generating an extensor moment at the ankle (plantarflexion), knee, and hip. As the surface becomes more vertically oriented, the force required is still vertical but because of the orientation change of the animal this becomes a progressively more caudally directed force. This is achieved by fixing the foot to the surface and generating a flexor moment at the ankle (dorsiflexion) and hip but an extensor moment at the knee. Thus, it might be expected that if climbing behavior was important in dromaeosaurids, a functional switch leading to a more important role for the flexor muscles (particularly around the foot, ankle, and hip) would have occurred, as has been observed in extant scansorial birds (Stolpe, 1932; Moreno, 1991). Myological analyses of extant climbing birds have demonstrated that the hindlimb flexors are stronger and better-developed than the extensors (Raikow, 1994). The caudodorsal shift of the pubis coupled with a knee-based flexor system (Gatesy, 1990) in maniraptoran theropods likely marks this switch from extensor to flexor muscles in the hind limb. Adaptation in hind limb flexor muscles would have also assisted deployment of the recurved claws in climbing and prey capture.

The evidence suggests that the form and resultant function of the "killer claws" was adapted to assist prey capture. All predators have to be adept at hunting, capturing, and killing (McFarland et al., 1979). Dromaeosaur claw geometry appears functionally adapted for prey capture, not for killing. In the light of earlier experimental results (Manning et al., 2006) and this study, it is possible to review the interpretation of the unique fossil (Fig. 7) of a *Velociraptor* and *Protoceratops* (Kielan-Jaworoska and Barsbold, 1972).

The remarkable fossil of the dromaeosaur *Velociraptor* entangled with an herbivorous dinosaur, *Protoceratops* (IGM 100/25), often called the "fighting pair" (Carpenter, 1998), may give some insight into claw function. The pair was collected from the Djadokhta Formation (Late Cretaceous) of Mongolia (Kielan-Jaworoska and Barsbold, 1972) and has caused much debate as to how the two came to be preserved together (Barsbold, 1974; Osmólska, 1993; Unwin et al., 1995; Carpenter, 1998). This unique fossil possibly shows a fatal stalemate, with the predators right leg pinned under the prey's body, the left foot hooked into the throat region and its right arm held in the jaws of its prey. The relative position of the predator's ensnared limbs meant it was pulled close to its prey and trapped. Unable to reposition its limbs, it was impossible for the *Velociraptor* to deploy its jaws and finish the attack, like two boxers hugging each other and unable to throw a punch.

Flexor tendon adaptations in the foot of *Velociraptor* might have contributed to the fatal embrace. The tendons (medius flexor digitorum longus) that flex the toes of extant perching birds are modified so that they lock the foot in a tight grip (McFarland et al., 1979). This grip is a result of specialized tendons that possess a ratchet-like mechanism in their sheaths, whereby numerous small projections on each tendon engage the ridges on the adjacent walls of the sheath (Welty, 1975). This allows birds to relax and sleep whilst perched, without releasing their grip and falling. The weight of the bird is enough to engage this elegant system. The underlying flexor tendons on the feet of dromaeosaurs might have possessed a similar ratchet-like "locking" mechanism on the second toe. The possession of such flexor tendons would have been an energy-efficient way of countering the effect of the claw's retractor ligament. They would have provided a useful adaptation for climbing and holding onto their prey, using gravity and limb position to assist the claw flexor and gripping function. The mechanism would then rely upon the dromaeosaur lifting its foot to release the underlying tendons to allow the retractor ligament to free the recurved claw from its prey; a dromaeosaur trapped/hugged by its prey would be unable to do so.

There is evidence for a large flexor system in *D. antirrhopus* (AMNH 2136), *Velociraptor mongoliensis* (AMNH 6518), and *Sinornithoides youngi* (Norell and Makovicky, 1997). Halfway down the caudo-ventral surface of metatarsal II, a robust longitudinal ridge (displaced slightly to the medial side) closely resembles the medial plantar crest of the avian metatarsus. Norell and Makovicky (1997) suggest this ridge might have functioned as an attachment site for the flexors and adductors of digits I and II, or possibly as a border that channeled flexor tendons. The plantar crest on the tarsometatarsus is well developed in raptorial and some species of swimming birds, which use their feet for propulsion. The medial plantar crest of the tarsometatarsus in some species of raptorial bird has become so enlarged that it almost encases the powerful flexor tendons. If the longitudinal ridge observed on the caudal face of the dromaeosaur metatarsus correlates to the medial plantar crest of birds, it seems likely to have served a similar function.

Farlow et al., (2000) noted that theropods more closely related to birds (including dromaeosaurs) show skeletal features indicative of a reduction in caudofemoral musculature. If the function of the recurved claw on the second toe was to disembowel prey, it seems illogical that limbs evolve to become progressively weaker. However, Norell and Makovicky (1999) noted that two specimens of *V. mongoliensis* possessed a fourth trochanter (proximal ridge of bone projecting from the medial shaft of the femur). Given that this is the attachment site for the main limb retractor, the caudofemoralis, this suggests that *V. mongoliensis* still employed this muscle.

CONCLUSIONS

The maximum value of stress generated by the FEM under the assumed loading conditions (400N) was around 60 MPa. The failure stress of extant claws (150–200 MPa) was significantly higher, suggesting that *Velociraptor* would have been able to support its weight on a small contact area while climbing.

The reversed hallux (Ostrom, 1969) of dromaeosaurs is now reconstructed so that this reduced digit was positioned craniolaterally and high on the metatarsus (Norell and Makovicky, 1999), a position that would functionally assist in climbing behavior.

We suggest that the anatomy, form, and function of digit II and manus claws of dromaeosaurs support the hypothesis of a prey capture/grappling/climbing function. This is supported by the homologous structures observed in the feet of modern perching/climbing birds. The geometry of dromaeosaur claws would have caused the claw to rotate as it was pushed deeper into prey which would have resulted in a maximum depth of trauma equal to the radius of the inside arch of the claw. The feet and hands of dromaeosaurs functioned both for locomotion (walking, running, and climbing) and as prey capture/grappling devices. We speculate that a ratchet-like "locking" ligament might have provided an energy-efficient way for dromaeosaurs to hook their recurved digit II claws into their prey, using body weight to lock the claws passively and allowing the jaws to dispatch prey.

ACKNOWLEDGMENTS

The X-ray tomography described in this article was carried out within the Stress and Damage Characterisation Unit within the School of Materials. They thank Dr Jonathon Codd (University of Manchester) for the use of the image in Fig. 7. The authors wish to thank Eric Snively, Peter Dodson, Eric Morschhauser and one anonymous reviewer for the helpful comments on the manuscript.

LITERATURE CITED

Alexander, R. McN. 1981. Factors of safety in the structure of animals. Sci Prog 67:109–130.

Alexander RM. 1989. Dynamics of dinosaurs and other extinct giants. New York: Columbia University Press. p 167.
Babout L, Mummery PM, Marrow TJ, Tzelepi A, Withers PJ. 2005. The effect of thermal oxidation on polycrystalline graphite studied by x-ray tomography. Carbon 43:765–774.
Barsbold R. 1974. Duelling dinosaurs. Priroda 2:81–83. [in Russian].
Beaupré GS, Carter DR. 1992. Finite element analysis in biomechanics. In: Biewener AA, editor. Biomechanics: structure and systems: a practical approach. New York: IRL Press. p 149–174.
Bonser RHC. 2000. The Young's modulus of ostrich claw keratin. J Mater Sci Lett 19:1039–1040.
Carpenter K. 1998. Evidence of predatory behaviour by carnivorous dinosaurs. In: Pérez-Moreno BP, Holtz TR, Sanz JL, Moratalla JJ, editors. Aspects of theropod palaeobiology. Gaia 15:135–144.
Carter DR, Hayes WC. 1977. The compressive behaviour of bone as a two-phase porous structure. J Bone Joint Surg 59A:954–962.
Chatterjee S. 1997. The rise of birds: 225 million years of evolution. London: The John Hopkins Press Ltd. p 312.
Clark JM, Norell MA, Chiappe LM. 1999. An oviraptorid skeleton from the late cretaceous of Ukhaa Tolgod, Mongolia, preserved in an avianlike brooding position over an oviraptorid nest. Am Mus Novit 3265:1–35.
Dominguez-Bellom G, Michelangeli F, Ruiz, MC, Garcia A, Rodriguez E. 1994. Ecology of the folivorous hoatzin (*Opisthocomas hoazin*) on the Venezuelan plains. Auk 111:643–651.
Elliott JC, Dover SD. 1982. X-ray microtomography. J Microsc 126:211–213.
Farlow JO, Gatesy SM, Holtz TR, Hutchinson JR, Robinson JM. 2000. Theropod locomotion. Am Zool 40:640–663.
Feduccia A. 1993. Evidence from claw geometry indicating arboreal habits of Archaeopteryx. Science 259:790–793.
Fraser RDB, MacRae TP. 1980. Molecular structure and mechanical properties of keratins. In: Vincent JFV, Currey JD, editors. The mechanical properties of biological materials. Cambridge: Cambridge University Press. 1968. pp. 211–246.
Gatesy S. 1990. Caudofemoral musculature and the evolution of theropod locomotion. Paleobiology 16:170–186.
Holtz TR, Osmólska H, Saurischia. 2004. In: Weishampel B, Dodson P, Osmólska H, editors. The Dinosauria. 2nd ed. Berkley: University of California Press. pp. 21–24.
Kak AC, Slaney M. 1987. Principles of computerized tomographic imaging. New York: IEEE Press.
Kanari M, Tanaka K, Baba S, Eto M. 1997a. Nanoindentation behavior of a two-dimensional carbon-carbon composite for nuclear applications. Carbon 35:1429–1437.
Kanari M, Tanaka K, Baba S, Eto M, Nakamura N. 1997b. Nanoindentation test on electron beam-irradiated boride layer of carbon-carbon composite for plasma facing component of large Tokamak device. J Nucl Mater 244:168–172.
Kielan-Jaworoska Z, Barsbold R. 1972. Results of the Polish-Mongolian paleontological expedition, Part IV. Acta Paleontol Pol 27:5–13.
Kitchener A, Vincent JFV. 1987. Composite theory and the effect of water on the stiffness of horn keratin. J Mater Sci 22:1385–1389.
Manning PL, Payne D, Pennicott J, Barrett P. 2006. Dinosaur killer claws or climbing crampons? Royal Soc Biol Lett 2:110–112.
Marrow TJ, Buffiere JY, Withers PJ, Johnson G, Engelberg D. 2004. High resolution x-ray tomography of short fatigue crack nucleation in austempered ductile cast iron. Int J Fatigue 26:717–725.
Matthew WD, Brown B. 1922. The family Deinodontidae, with notice of a new genus from the cretaceous of Alberta. Bull Am Mus Nat Hist 46:367–385.
McFarland WN, Pough FH, Cade TJ, Heiser JB. 1979. Vertebrate life. New York: MacMillan Publishing. p 875.
Moreno E. 1991. Musculature of the pelvic appendages of the tree creepers (Passeriformes: Certhiidae): mycological adaptations for tail-supported climbing. Can J Zool 17:191–209.
Norell M, Makovicky PJ. 1997. Important features of the dromaeosaur skeleton: information from a new specimen. Am Mus Novit 3215:1–28.
Norell M, Makovicky PJ. 1999. Important features of the dromaeosaur skeleton. II. Information from newly collected specimens of *Velociraptor mongoliensis*. Am Mus Novit 3282:1–45.
Norell M, Makovicky PJ. 2004. Dromaeosauridae. In: Weishampel B, Dodson P, Osmólska H, editors. The Dinosauria. 2nd ed. Berkley: University of California Press, 862. pp 196–209.
Osborn HF. 1924. Three new theropoda, *Protoceratops* zone, central Mongolia. Am Mus Novit 144:1–12.
Ostrom JH. 1969. Osteology of *Deinonychus antirrhopus*, an unusual theropod from the lower cretaceous of Montana. Bull Peabody Mus Nat Hist 30:165.
Ostrom JH. 1990. Dromaeosauridae. In: Weishampel B, Dodson P, Osmólska H, editors. The Dinosauria. First edition. Berkley: University of California Press, pp 269–279, 733.
Osmólska H. 1993. Were the Mongolian "fighting dinosaurs" really fighting? Paléobiology (Spec Vol) 7:161–162.
Pennisi E. 2005. Birds wings really are like dinosaurs' hands. Science 307:194–195.
Penteriani V, Gallardo M, Roche P. 2002. Landscape structure and food supply affect eagle owl (*Bubo bubo*) density and breeding performance: a case of intra-population heterogeneity. J Zool 257:365–372.
Raikow RJ. 1994. Climbing adaptations in the hindlimb musculature of the wood creepers (Dedrocolaptinae). Condor 96:1103–1106.
Raven PH, Johnson GB. 1992. Biology. 3rd ed. St. Louis, Missouri: Mosby Year Book. p 1217.
Stolpe M. 1932. Physiologisch-anatomische untersuchungen über die hintere extremität der vögel. J Ornithol 80:161–247.
Sues HD. 1977. The skull of *Velociraptor mongoliensis*, a small Cretaceous theropod dinosaur from Mongolia. Palaeontologische Zeitschrift 51:173–184.
Unwin DM, Perle A, Trueman C. 1995. *Protoceratops* and *Velociraptor* preserved in association: evidence for predatory behaviour in dromaeosaurid dinosaurs. J Vertebr Palaeontol (Abstracts of papers, fifty-fifth Annual Meeting) 15 (suppl 3):57A.
van Ruijven LJ, Giesen EBW, van Eijden TMGJ. 2002. J Dent Res 81:706–710.
Vargos AO, Fallon JF. 2004. Birds have dinosaur wings: the molecular evidence. J Exp Zool 304:1–5.
Vincent JFV, Owers P. 1986. Mechanical design of hedgehog spines and porcupine quills. J Zool 210:55–75.
Welty JC. 1975. The life of birds. 2nd ed. Philadelphia: Saunders WB. 623 p.
Witmer LM. 1995. The extant phylogenetic bracket and the importance of reconstructing soft tissue in fossils. In: Thomason JJ, editor. Functional morphology in vertebrate palaeontology. Cambridge: Cambridge University Press. pp 19–33.
Youssef S, Maire E, Gaertner R. 2005. Finite element modelling of the actual structure of cellular materials determined by x-ray tomography. Acta Mater 53:719–730.